IEEE Photonics Journal
An IEEE Photonics Society Publication

Open Access

Why Do Field-Based Methods Fail to Model Plasmonics?

Volume 8, Number 5, October 2016

A. M. A. Said
A. M. Heikal
Nihal F. F. Areed
S. S. A. Obayya

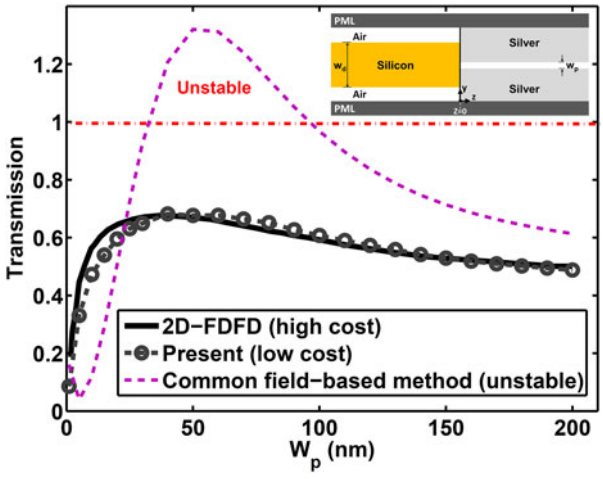

DOI: 10.1109/JPHOT.2016.2600367
1943-0655 © 2016 IEEE

Why Do Field-Based Methods Fail to Model Plasmonics?

A. M. A. Said,[1,2] A. M. Heikal,[1,2] Nihal F. F. Areed,[1,2] and S. S. A. Obayya[2]

[1]Electronics and Communications Engineering Department, Faculty of Engineering, Mansoura University, Mansoura 35516, Egypt
[2]Center for Photonics and Smart Materials, Zewail City of Science and Technology, Giza 12588, Egypt

DOI:10.1109/JPHOT.2016.2600367

Manuscript received July 14, 2016; revised August 8, 2016; accepted August 10, 2016. Date of publication August 15, 2016; date of current version September 30, 2016. This work was supported by the National Telecom Regulatory Authority, Egypt (http://www.ntra.gov.eg) to demonstrate the theoretical study proposed in this work. Corresponding author: S. S. A. Obayya (e-mail: sobayya@zewailcity.edu.org).

Abstract: The paper studies plasmonics modeling issues and examines the reasons behind the failure of the field-based methods relying on Padé approximations widely used in the analysis of photonic devices based on dielectric materials. Through a study of evanescent, radiation, guided, and surface modes of a plasmonic structure where the failure appears clearly, we demonstrate the physical explanation of this failure and suggest some remedies. We developed a Bidirectional Beam Propagation Method (BiBPM) by adopting a Blocked Schur (BS) algorithm to introduce an unconditionally stable method for plasmonic structures with strong discontinuities. Central to BiBPMs is the accurate calculation of the square root operators that is very widely performed using Padé approximations. However, recent reports demonstrate convergence of Padé that is too slow to lend itself a stable solver in plasmonics [1]. Moreover, Padé approximations completely fail in handling such a strong discontinuity between dielectric and plasmonic waveguides, where a very-wide spectrum of modes could be excited. Alternatively, we propose calculating these operators by the twice faster BS algorithm. Beyond the computational speed, our suggested approach overbears the Padé-based BiBPMs instability and accuracy problems, thanks to the proper physical treatment of surface and evanescent waves: the notorious sources of instability. Through the plasmonic discontinuity problems, the superiority of BS approach has been determined numerically and explained physically.

Index Terms: Bidirectional Beam Propagation Method (BiBPM), blocked schur, dielectric waveguides, high-index-contrast discontinuity, plasmonic coupler, plasmonic waveguides, plasmonics modeling.

1. Introduction

Plasmonic devices are currently key components in high density integrated photonic circuits [2], [3]. However, modeling optical waveguides with strong longitudinal and transverse discontinuities like in plasmonic devices remains a defiance facing numerical techniques. Such strong discontinuities as those encountered in couplers between dielectric and plasmonic waveguides lead to the excitation of a large number of radiation, evanescent, and surface modes. In this case, accurate treatment of all this wide spectrum of modes becomes extremely difficult or impossible to predict a physically correct model for such hybrid dielectric-plasmonic devices. Despite the versatility of time domain techniques

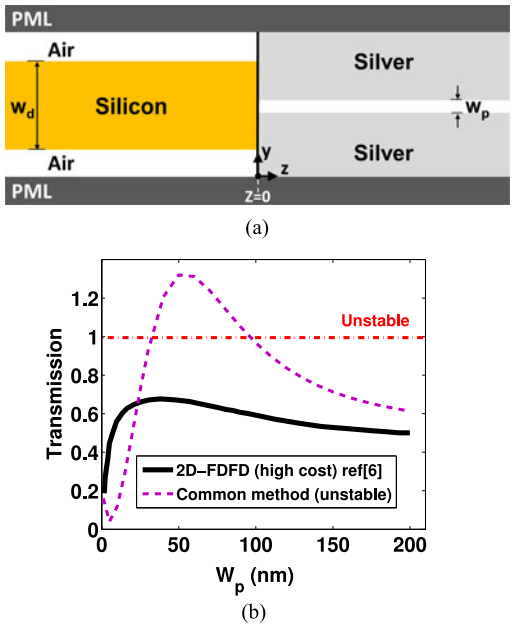

Fig. 1. (a) Schematic diagram of a coupler between a dielectric and a plasmonic waveguide showing very-high-index-contrast longitudinal and transverse discontinuities. The fundamental TM mode is excited in the dielectric waveguide with width of $W_d = 300$ nm at wavelength 1550 nm. (b) Coupler transmission efficiency as a function of the plasmonic waveguide width (W_p). Unstable results are calculated using the commonly-used Padé approximation [6] and compared with the accurate results reported in [5] using 2D-FDFD, which required very high computational cost.

such as finite difference time domain method (FDTD), they suffer from two salient problems. It is well known that time-domain analysis is very computationally intensive [4]. Moreover, it is very difficult to cast a model which can accurately describe the metals dispersion at optical frequencies. Approximating the relative permittivity (ϵ_r) of metals by a model, such as Drude or Drude-Lorent models, and integrating such models with time-domain analysis are very complex processes. The produced auxiliary equations from such models may cause serious numerical instability and lead to extra computational efforts. Therefore, when it comes to plasmonics, the frequency domain techniques, for instance, the field based methods [5]–[11] and the modal based methods [12], are more effective and attractive in terms of computational time and memory. Furthermore, frequency domain methods permit to directly use metals experimental relative permittivity ϵ_r with no further approximations or complication. However, the precision of modal based methods [12] relies hardly on the number of radiation and guided modes which are unduly difficult while dealing with surface plasmon polariton structures (SPPs). For example, about 60 eigenmodes have to be searched in a complex plane to find evanescent modes, radiation modes, and guided modes of a SPP structure while using complex mode matching method (CMMM) [12]. Moreover, treating problems with such strong discontinuities in plasmonics with Finite Element Methods (FEM) or finite difference frequency domain methods (FDFD) [5] needs to divide the discontinuity surfaces into smaller elements and hence increases the computational costs and projection errors associated with mesh discretization. For instance, the two-dimensional FDFD (2D-FDFD) relies on meshing the whole computational domain with 2D elements and requires higher-order differences to successfully treat plasmonics. In [5], the forth order of 2D-FDFD had to be used to accurately analyze the plasmonic coupler investigated there shown in Fig. 1(a). Despite 2D-FDFD efficiency introduced with SPPs [5], as shown in Fig. 1(b), its computational efforts are expensive and will increase excessively with the size of the structure, the number of discontinuities. However, other field based methods [6]–[9], [13], [14], such as BiBPM [7], are known for their efficiency, simplicity, and numerical speed for the analysis of dielectric based devices; however, none of these methods is efficient for the analysis of

plasmonic based devices [1], [11], as shown in Fig. 1. Therefore, this paper examines the physical reasons behind the instability of field-based methods and focuses on the role played by evanescent modes in this issue. In addition, the motivation of this work is to keep the computational effort minimum with little dependence on the size of the structure, the number of discontinuities in the propagation direction, through developing a new type of BiBPMs able to efficiently treat plasmonic based devices.

All previously introduced types of field-based methods [6]–[9], [11], [13], [14] rely mainly on approximating the square root operators of the structure characteristic matrix utilizing iterative methods [6], [8]–[10], [15], [16]. Although the iterative methods such as Padé approximations [6], [8], [16] are widely-utilized in dielectric structures, they sustain instability while considering very high-index-contrast discontinuities as shown in Fig. 1 in SPPs, as the fit modeling of the evanescent waves begins to be climacteric, and their conventional treatment techniques [6], [8], [9], [11] almost fail. On the other hand, the exact solutions of these square root operators could be obtained by direct methods [15], [16]. The Schur method, as an example of direct methods, is the most numerically stable method [15] owing to Schur decomposition which produces all eigenvalues of the characteristic matrix of the structure. Thus, evanescent, radiation, and guided modes could be efficiently modeled even in SPPs. Despite the high precision of direct methods, they have never been applied for plasmonic devices because they demand massive computational resources for both memory and time.

In this work, Blocked Schur (BS) [17] has to be exploited for high-index-contrast discontinuities in SPPs to attenuate all shortcomings of both direct and iterative methods. BS is an improved version of Schur method (about six times faster) [17]. Its speedup is owing to more efficient use of cache memory during computing blocks square root of the upper triangular matrix by a superdiagonal or a column at once. Moreover, iterative methods might be slower than BS when high-order approximations are required. Furthermore, acceleration of 3D structures analysis could be achieved through BS capability of parallel implementation [17]. In [18], we developed the so-called Blocked Schur-Finite Element-Bidirectional Beam Propagation Method (BS-FE-BiBPM) to solve the 2D time-independent Schrödinger equation for electron waveguides based devices. The method is particularly efficient for analyzing electron waveguide discontinuity problems such as in a quantum waveguide transistor consuming only few seconds compared to multiple hours of time domain techniques.

In this paper, we demonstrate a study for the physical explanation of the instability of field-based methods from evanescent modes in SPPs through analyzing a coupler between a dielectric and a plasmonic waveguide (plasmonic coupler) in Section II. Based on this study, we suggest adopting BS with branch-cut technique [6], [19] instead of the widely-used Padé approximation to stabilize BiBPM with plasmonics. We actually introduce an unconditionally stable method for plasmonics by extending BS-FE-BiBPM to solve the 2D Helmholtz equation for optical waveguides with very-high-index-contrast discontinuities. A brief description of this stabilized BiBPM is given in Section III. As a further evidence of the efficiency of our stabilized BiBPM, a long rang surface plasmon polariton structure (LR-SPP) is analyzed in Section IV. Its calculations have excellent agreement with experimental data. All numerical results in the paper are introduced through a study of accuracy, stability and computational cost of both approaches based on the suggested BS and the conventional Padé approximations. Then, a conclusion will be drawn.

2. Physical Explanation of Instability

As a clear instance of the failure of conventional field-based methods with plasmonics, we study the plasmonic coupler [5], shown in Fig. 1(a), as an example for a single discontinuity between dielectric and plasmonic waveguides with very-high-index-contrast. The major challenge of such structure is to deal correctly with the extensive number of evanescent and radiation modes excited by the strong discontinuity between the dielectric and plasmonic waveguides in this plasmonic coupler. The dielectric constant of silicon and the experimental data of silver are directly adopted from [20].

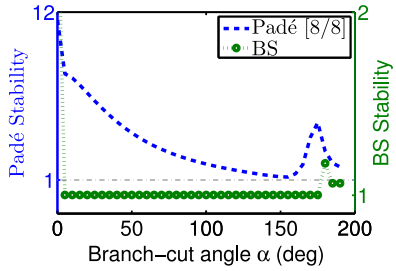

Fig. 2. Power stability versus α at $W_p = 10$ nm of rotated-complex Padé [8/8] and the suggested method based on the Blocked Schur (BS) algorithm.

2.1. Evanescent Modes

It is well known that a unique square root of a matrix is exist, only if the matrix is positive definite. If the matrix has some negative eigenvalues on R^-, that is called the nonprincipal square root [15]. The existence of these negative eigenvalues on R^- directly refers to the evanescent modes. Fortunately, for matrices with semi-simple zero eigenvalues on R^-, such as dielectric waveguides with low-index-contrast, Schur methods are able to automatically handle these evanescent modes without any treatment techniques, while the iterative methods cannot. Moreover, introducing the characteristic matrix eigenvalues via Schur decomposition makes BS more efficient to suppress all the evanescent modes. However, the branch-cut technique [6], [19] is required before applying BS to efficiently suppress the evanescent modes in matrices with large negative eigenvalues on R^- like in SPPs with very-high-index-contrast. Utilizing branch-cut is to produce a new rotated characteristic matrix $[A]_i$ for each waveguide i

$$\sqrt{[A]_i} = e^{j\alpha/2}\sqrt{[A]_i e^{-j\alpha}} \tag{1}$$

in which the original real axis has to be rotated by an angle α. Furthermore, BS displays excellent stability with any branch-cut angle $\alpha \in]0^\circ, 180^\circ[$, while the iterative methods are perhaps unsuccessful (see Fig. 2). Fig. 2 shows the stability of both rotated-complex-Padé [8/8] and the suggested method based on BS in the case of $W_p = 10$ nm while changing the branch-cut angle α. Although Padé approximation shows complete instability along all angles, neither the stability nor the accuracy of the suggested BS method have been affected by α in the range $]0^\circ, 180^\circ[$, as shown in Fig. 2. BS excellent stability is due to its mathematical ability to represent all the eigenvalues of the characteristic matrix in the diagonal of the triangular matrix produced by Schur decomposition. As a result, all the excited spectrum of the evanescent, radiation, and surface waves could be efficiently handled.

Therefore, a study of eigenmodes [21] and its stability conditions is needed to help to deeply understand the reasons of Padé instability shown in Figs. 1(b) and 2. Therefore, we examine the eigenvalues (β) and its square root ($\sqrt{\beta}$) of TM characteristic matrix of the plasmonic waveguide $[A]_2$ at two cases: $W_p = 50$ nm and 200 nm as samples for unstable and quasi-stable regions of Padé, respectively, as noticed in Fig. 1(b). β and $\sqrt{\beta}$ are directly proportional to the square of the effective refractive index n_{eff}^2 and n_{eff}, respectively. In addition, $\sqrt{\beta}$ can be classified into four domains, as shown in Fig. 3. The nonprincipal square root directly leads to physical and nonphysical evanescent modes located in domains I and II, respectively. The propagating modes have positive Re(β) with positive Im(β); thus, they are located in domain III. Domain IV contains the highly lossy modes which have positive Re(β) and large positive Im(β). The classification of modes and their locations in the four domains are stated in Table I according to Re(β) and Im(β).

Mainly, two problems are responsible for the instability issue. The first problem arises when Re(β) is negative which is defined as the nonprincipal square root. Second problem is when Im(β) is negative, then, serious evanescent modes appears. The branch-cut technique could overcome these two problems, only if it could rotate all set of β to have both positive real and imaginary parts (Domain III). However, in some cases, there is no angle could rotate all modes without remains. Moreover,

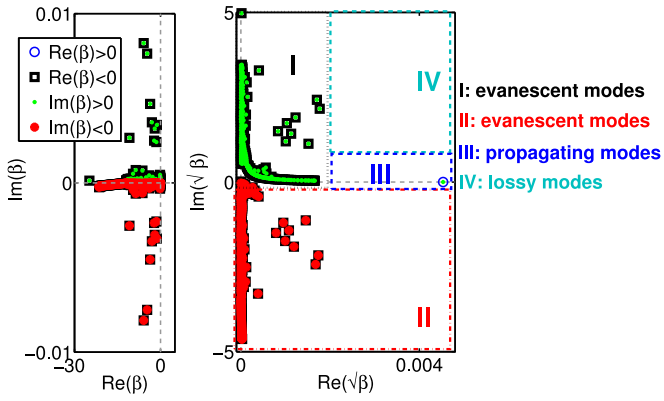

Fig. 3. Set of eigenvalues (β) of $[A]_2$ and their modes classification and locations.

TABLE I

Classification of Modes and Their Locations in the Four Domains Shown in Fig. 3

Mode type	evanescent	evanescent (worst)	propagating	lossy
Re(β)	<0	<0	>0	>0
Im(β)	$>=0$	<0	$>=0$	>0 (larger)
$\sqrt{\beta}$ location	Domain I	Domain II	Domain III	Domain IV

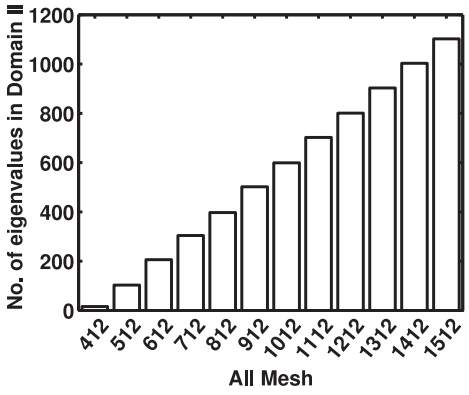

Fig. 4. Number of eigenvalues in the lower half of the complex plane, particularly in domain II, of characteristic matrix of the plasmonic waveguide with $W_p = 50$ nm before using branch-cut and while increasing the mesh in the core layer by 100 elements and fixing the mesh outside the core to 394 elements. Starting from the mesh of 512 elements, any increase of the core mesh, 100 elements here, reflects directly to the same increase in the number of eigenvalues in domain II, which is also 100 eigenvalues here. Therefore, we can consider the majority of these modes in domain II as nonphysical modes.

the worst case of stability issue occurs when β of these remains suffers from the two problems together, negative Re(β) with negative Im(β), (Domain II). Although a huge number of modes in domain II, before branch-cut, is nonphysical modes related to the mesh as examined in Fig. 4, after branch-cut rotation domain II may contain the main physical modes which cannot be reduced or suppressed.

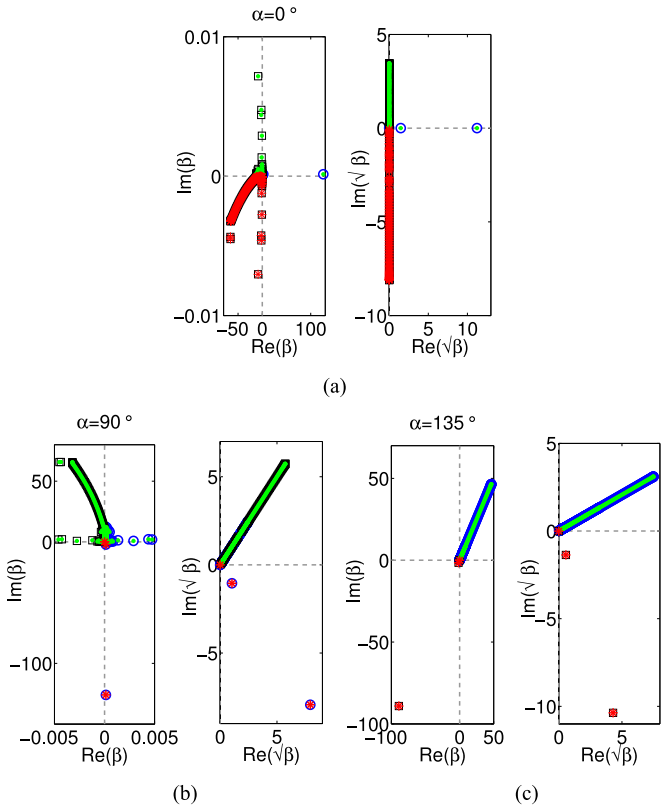

Fig. 5. Complete set of β and $\sqrt{\beta}$ of $[A]_2$ at $W_p = 50$ nm (unstable case). (a) Before, applying branch-cut technique $\alpha = 0^\circ$, (b) after applying branch-cut technique with $\alpha = 90^\circ$, and (c) with $\alpha = 135^\circ$.

TABLE II

Number of Modes Located in Each Domain Before and After Branch-Cut for the Unstable Case of $[A]_2$ at $W_p = 50$ nm and Representing Worst Mode by Minimum Re(β) and Minimum Im(β)

	$\alpha = 0^\circ$	$\alpha = 90^\circ$	$\alpha = 135^\circ$
min(Re(β))	> -70	> -0.008	> -100
min(Im(β))	> -0.01	> -150	> -100
Domain I	406	103	0
Domain II	103	3	3
Domain III & IV	3	406	509

2.1.1. Unstable Case: $W_p = 50$ nm: Fig. 5(a) displays β and $\sqrt{\beta}$ without branch-cut ($\alpha = 0^\circ$) for the plasmonic characteristic matrix when $W_p = 50$ nm. The nonprinciple square root is clear in Fig. 5(a) and Table II, where about 406 and 103 evanescent modes appear in domains I and II, respectively. Moreover, there are three modes still appear in domain II while changing α from 90° in Fig. 5(b) to 135° in Fig. 5(c). Unfortunately, there is no angle from 0° to 180° could reduce the existence of modes in domain II. In addition, some of these modes suffer from the two problems together (large negative Re(β) and large negative Im(β)), as summarized in Table II. In addition, the big differences between the modal sizes of the dielectric mode of $W_d = 300$ nm and the plasmonic

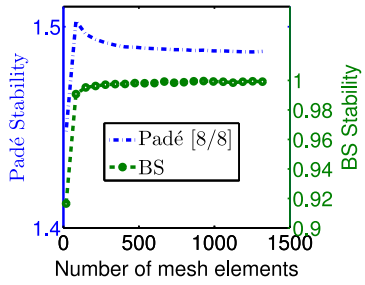

Fig. 6. Convergence study for the power stability with mesh at $W_p = 50$ nm of rotated-complex Padé [8/8] and the suggested method based on Blocked Schur (BS) algorithm.

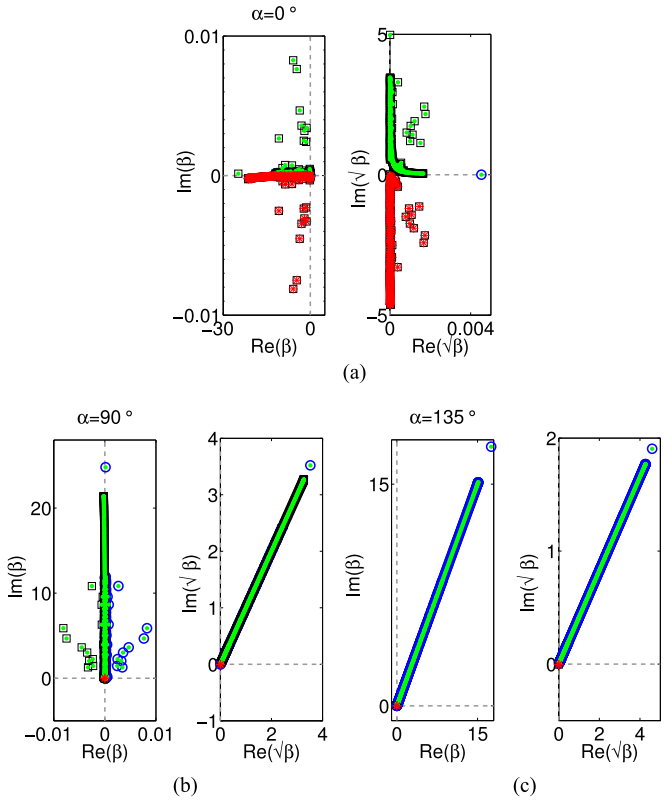

Fig. 7. Complete set of β and $\sqrt{\beta}$ of $[A]_2$ at $W_p = 200$ nm (Quasi-stable case). (a) Before applying branch-cut technique $\alpha = 0^\circ$, (b) after applying branch-cut technique with $\alpha = 90^\circ$, and (c) with $\alpha = 135^\circ$.

mode of $W_p = 50$ nm plays a big role in exciting this large number of radiation, evanescent, and surface modes at such strong mismatch. That is why Padé shows serious instability in Fig. 1(b), especially at $W_p = 50$ nm. In order to study the convergence of the proposed method, a convergence study versus number of mesh elements has been added for the structure shown in Fig. 1(a), where W_p is fixed to 50 nm. Fig. 6 shows that the proposed method converges into the stable value 1, even for a small number of mesh elements while the Padé converges into unstable power value.

2.1.2. Quasi-Stable Case: $W_p = 200$ nm: Fig. 7 and Table III present the case of $W_p = 200$ nm. Fig. 7(a) displays β and $\sqrt{\beta}$ without branch-cut ($\alpha = 0^\circ$), where about 301 and 200 evanescent modes appear in domains I and II, respectively. However, it could be noticed that this matrix has much smaller negative Re(β). $\alpha = 90^\circ$ rotates all set of β to have smaller negative Re(β) and positive Im(β), except one mode (a better case of the nonprincipal square root). This mode appears in domain II, as shown in Fig. 7(b). Therefore, Padé stability starts to converge as shown

TABLE III

Number of Modes Located in Each Domain Before and After Branch-Cut for the Quasi-Stable Case of $[A]_2$ at $W_p = 200$ nm and Representing Worst Mode by Minimum Re(β) and Minimum Im(β)

	$\alpha = 0^\circ$	$\alpha = 90^\circ$	$\alpha = 135^\circ$
min(Re(β))	> -30	> -0.01	$> -1.5 \times 10^{-5}$
min(Im(β))	> -0.01	$> -3 \times 10^{-5}$	$> -1.5 \times 10^{-5}$
Domain I	311	200	0
Domain II	200	1	1
Domain III & IV	1	311	511

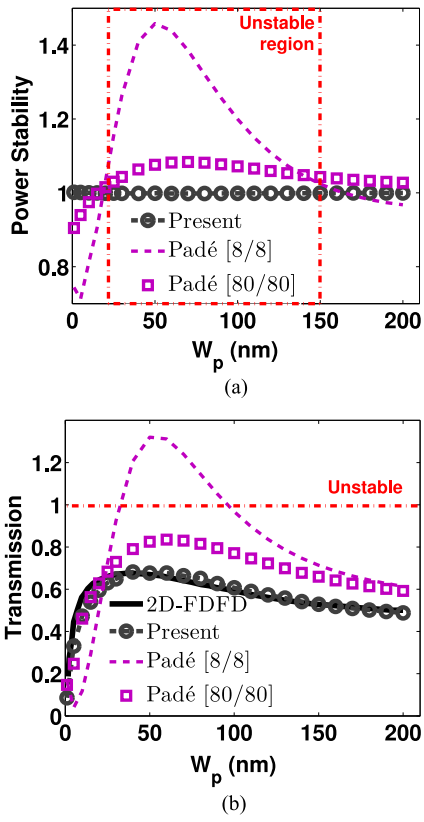

Fig. 8. (a) Power stability (b) and transmission efficiency for the plasmonic coupler shown in Fig. 1(a) as a function of W_p.

in Fig. 8(a) at $W_p = 200$ nm. In addition, Fig. 7(c) shows that $\alpha = 135^\circ$ successes to rotate all set of β to have positive Re(β) and positive Im(β), except one mode. This remaining mode suffers from the two problems (negative Re(β) with negative Im(β)). Therefore, it also stays in domain II. From another point of view, the small mismatch between the modal sizes of $W_d = 300$ nm and $W_p = 200$ nm reduces the number of radiation, evanescent, and surface modes excited at such discontinuity. Moreover, the phase difference between the plasmonic and dielectric waveguides starts to decrease at larger W_p where the phase of the plasmonic waveguide decreases towards zero (the phase of any dielectric waveguide), i.e., the plasmonic waveguide with large W_p starts to

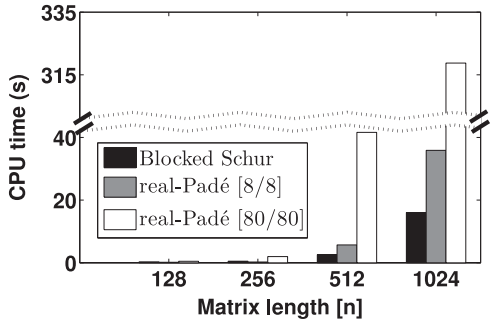

Fig. 9. Square root computational time of two full [n × n] matrices appearing at the discontinuity section in Fig. 1(a).

behave more like dielectric than plasmonic, and the plasmonic mode starts to seem more like the transverse electromagnetic (TEM) mode at such large W_p. As a result, it could be considered that we have a less challenging dielectric-to-dielectric discontinuity problem.

It could be summarized that besides the nonprincipal square root, the presence of modes in domain II is a main reason of the serious instability. These evanescent modes always appear when Im(β) is negative, and become difficult to be suppressed if Re(β) is also negative (the nonprincipal square root). Thus, a method which could rotate the maximum number of such modes and could deal correctly with the remains is the only way to get stable solutions. Therefore, for stability, we may have no choice but to use BS.

2.2. Reference Indexes

The commonly employed iterative methods to approximate $\sqrt{[A]_i} = k_0 n_{0,i}\sqrt{I + X_i}$ like Taylor expansion and Padé approximations are mathematically valid only if the absolute of the largest eigenvalue of $[X]$ is less than 1 [15]. Hence, the characteristic matrix $[A]_i$ might have to be expanded around a reference index $n_{\text{ref},i}$ and divided by $k_0^2 n_{\text{ref},i}^2$. Selecting a fit reference index is important to reduce errors as possible. That is why Padé approximations conventionally expand the characteristic matrix around the fundamental mode by its n_{eff}. Therefore, n_{ref} for the expansion is selected to equal to n_{eff} while studying the plasmonic coupler. We also studied the changing of n_{ref}; however, Padé is still unstable. Otherwise, the Schur algorithms capability of directly calculating the square root for general nonsymetric matrices [15] keeps away from any errors introduced by the characteristic matrix expansion around a chosen reference index. In other words, the Schur method, as well as BS, do not depend on any n_{ref}.

2.3. Order of Approximations and Computational Cost

It was reported in [6] that the combination of Padé types can present a good precision when α is greater than 45° and Padé order is greater than 6. Therefore, we implemented here rotated-complex-Padé [6] with higher-orders of [8/8] and $\alpha = 90°$ for the study shown in Fig. 8. However, Padé results of order [8/8] are still incorrect and unstable as shown in Fig. 8. That is why we attempted Padé orders higher than [8/8] until we reached [80/80]. However, it could be noted that when W_p is between 20 nm and 150 nm, Padé still shows a region of serious instability (Unstable case) as shown in Fig. 8(a). Also, where W_p is larger than 150 nm, Padé stability starts to converge but remains above one slightly (Quasi-stable case). Although the order [80/80] slightly lowers the instability, as shown in Fig. 8(a), its transmission calculations, in Fig. 8(b), remain incorrect while consuming extreme computational time as we can see in Fig. 9.

The computational cost of the two square root operators appearing at the discontinuity section $z = 0$ is introduced via BS and the lowest cost of Padé types (real-Padé). Fig. 9 shows BS reduction in the run time of calculating these operators. Serial implementation of BS could save ∼55% of the computational time compared with real-Padé of only order [8/8]. In addition, BS can save about two thirds of the execution time of Schur method [17].

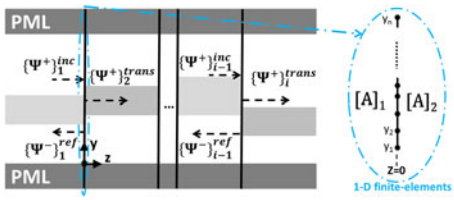

Fig. 10. Schematic diagram of optical waveguides with multiple longitudinal discontinuities $(i-1)$. The first discontinuity is located at $z=0$. $\{\psi^-\}_i$ and $\{\psi^+\}_i$ are the backward and forward propagating fields, respectively.

In other words, iterative methods may require as huge cost as that of Schur method ($28\frac{1}{3}n^3$ flops for $[n \times n]$ matrix), depending on the properties of the matrix and the desired accuracy, i.e., depending on the number of iterations required [15]. Unfortunately, Taylor expansion [9] needs more matrix multiplications, and Padé-type of higher order approximations requires more matrix inversions. Of course, for SPPs higher-orders of iterations are required to restrain any probable errors that might results in serious accuracy and stability problems. As a result, the iterative methods may be computationally intensive and still incorrect as we see in Figs. 8 and 9. Moreover, BS is better to speed up the calculation of these operators through using blocking technique since it permits more efficient use of cache memory [17]. However, Schur method takes long execution time while sweeping the matrix element by element, without making use of the cache memory, without any blocking. Therefore, for high numerical precision we recommend BS which would be faster especially with SPPs.

In addition, it is well known that numerical modeling of SPPs demands extremely smaller mesh size than modeling of low- or high-index-contrast dielectric structures to be able to resolve the field high localization at dielectric-metal interfaces of SPPs [22]. Such SPPs, operating around the optical communication wavelength, need a mesh size of 1 nm around interfaces [22], which, of course, requires huge computational resources. Therefore, using BS with SPPs can save simulation time. Moreover, BS algorithm can be implemented on a parallel platform hence achieving more reduction in computation time [17].

3. Stabilized BiBPM

For a general 2D optical discontinuity problem as shown in Fig. 10, we suppose that the transverse direction is assumed to be y with no variation in x-direction, and z is the direction of propagation. Each waveguide i could be governed by 2D Helmholtz equation [9]. The characteristic matrix $[A]_i$ of each waveguide i could be obtained by using finite difference or finite element method. Here, we use the standard Galerkin's finite-element procedure with first-order linear elements which results in

$$\frac{d^2\{\psi\}_i}{dz^2} + [A]_i\{\psi\}_i = \{0\} \tag{2}$$

where $[A]_i$ is characteristic matrix of waveguide i, $\{0\}$ is the null vector, and $\{\psi\}_i$ is the nodal field vector. We also use refractive index of metals as $n_m = n + Kj$. The formal solution of (2) for each waveguide i is written as

$$\{\psi\}_i(z) = \exp(+j\sqrt{[A]_i}z)\{\psi^+\}_i + \exp(-j\sqrt{[A]_i}z)\{\psi^-\}_i \tag{3}$$

where $\{\psi^-\}_i$ and $\{\psi^+\}_i$ are the backward and forward propagating fields, respectively, in each waveguide i at the discontinuity plane.

For treating multiple discontinuities like in Fig. 10 by BiBPMs, the square root operator $\sqrt{[A]_i}$ appears not only at transition steps when applying the continuity equations of the transverse magnetic and electric fields at each interface but at propagation steps, as well. Therefore, the stability of BiBPMs is very sensitive to the modeling of the evanescent waves in such operators.

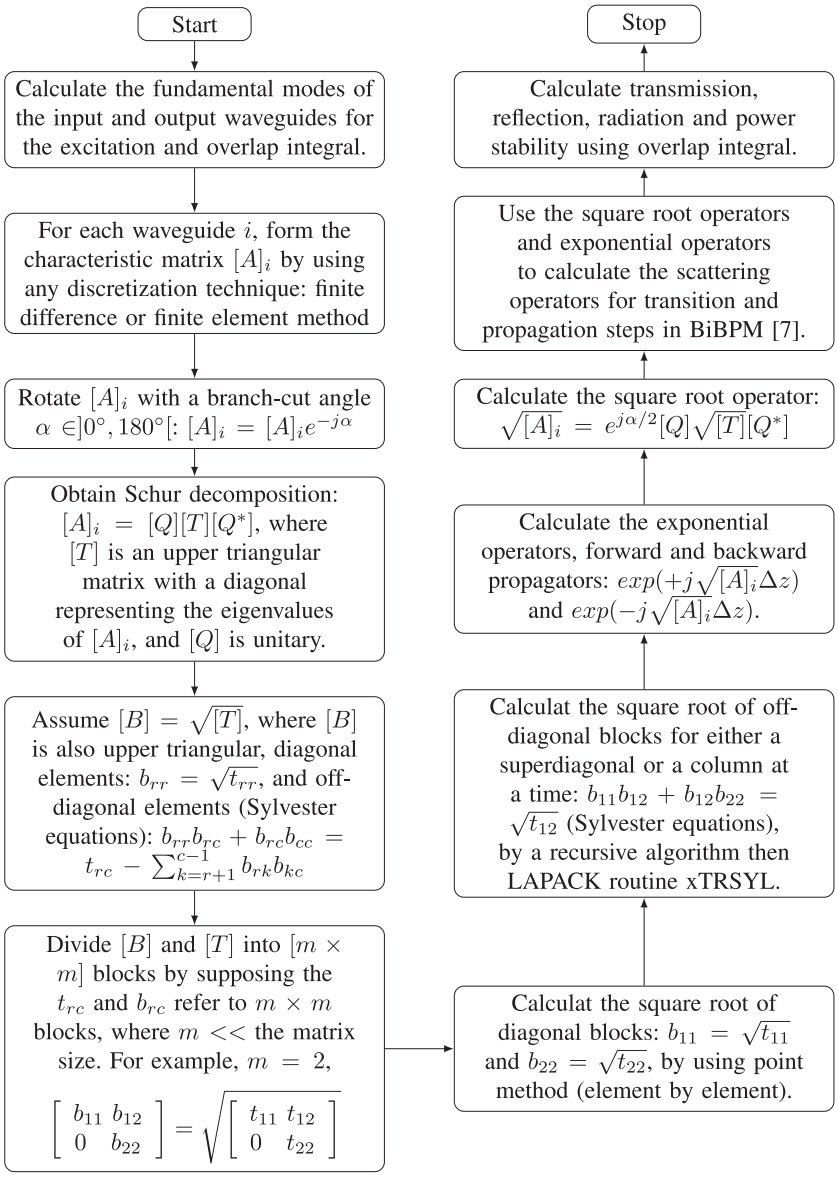

Fig. 11. Workflow of the whole algorithm of the stabilized BiBPM based on Blocked Schur.

Therefore, for plasmonics, we modified the BiBPM [7], which is efficient only with dielectric based devices, by using BS instead of the commonly-used Padé approximations. Fig. 11 describes the workflow of the whole algorithm of the stabilized BiBPM based on Blocked Schur. Adopting BS [17] overcomes instability issues of conventional BiBPMs based on Padé approximations while dealing with critical evanescent waves in SPPs. That is, owing to BS ability to efficiently calculate the exact solution of these square root operators with a diagonal of eigenvalues representing all modes excited.

4. Stabilized BiBPM Meets Experimental Data

4.1. LR-SPP

Another structure simulated is a LR-SPP shown in Fig. 12(a). Although it could be considered as a less challenging longitudinal discontinuities between plasmonic to plasmonic waveguides (less

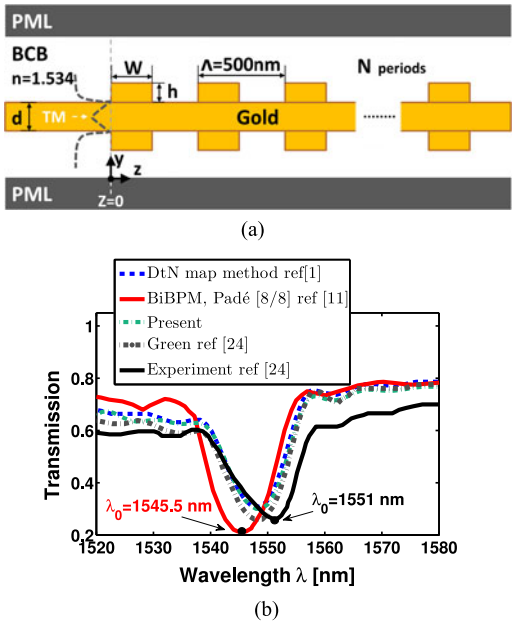

Fig. 12. (a) Schematic of the LR-SPP based Bragg grating structure. (b) Transmission for LR-SPP gratings with $N = 160$.

phase difference), it is an example of a very long structure ($80\,\mu$) with multiple discontinuities which will require huge computational cost in terms of time and memory while meshing the whole structure using FDTD, FEM, or 2D-FDFD. However, we make use of any repetitions of waveguides in structures. So, for the structure shown in Fig. 12(a) we need to calculate two square root operators and two propagators of only the two sides of the first discontinuity interface located at $z = 0$ as they will be repeated to the end of the structure. Then, we use matrices multiplications to represent the whole structure by repeating the transition and propagation steps. That makes the computational cost minimum and almost independent of the number of discontinuities.

The structure is with a grating period of $\Lambda = 500$ nm. For number of periods $N = 160$, Fig. 12(b) shows the transmission of the fundamental TM mode incident from $z = 0-$ as a function of the wavelength. To justify the comparison, we utilized the same refractive index for gold $n = 0.559 + 9.81i$ as in [1] and for BCB polymer $n = 1.534$. The presented results show excellent agreement with numerical methods such as the DtN map method [1], which matched very well with the integral equation method [23] and Green method [24]. Furthermore, the presented results show very good agreement with the experimental results reported in [24]. However, the published data calculated by the conventional BiBPM based on rotated-complex Padé approximation [11] shows a clear shift for the central wavelength (λ_0) compared with the experimental results. These shifted results could be noticed in Fig. 12(b) represented by the red solid line. Moreover, the DtN map method [1] has used rotated-Padé for the transition step only, while another more complicated marching technique based on DtN has to be introduced for the propagation instead of BiBPM to be able to efficiently provide damping for evanescent modes. That is due to the problem reported there of the slow convergence of branch cut angle with BiBPM based on Padé approximation for high-index-contrast structures [1]. Therefore, we suggest using BS instead of Padé approximations to make BiBPM efficient for high-index-contrast structures.

5. Conclusion

A study for the physical reasons behind the instability of the modeling methods based on the widely used Padé approximations has been demonstrated in this paper. As an alternative to Padé approximations, a stabilized BiBPM based on Blocked Schur (BS) has been developed for treating

very high-index-contrast transverse and longitudinal discontinuities in plasmonic structures. This suggested approach introduces an unconditionally stable method for plasmonics analysis. Unlike the widely-used Padé approximations, the proposed method shows excellent numerical stability with the capability of exactly handling the wide-spectrum of surface and evanescent waves. Beyond the numerical stability BS serial implementation reduced the computational time of matrix square root of size [1024 $\times$ 1024] by $\sim$55% compared with real-Padé of only order [8/8]. We also believe it is possible to extend our method to 3D full-vectorial analysis. Moreover, making use of BS parallel implementation should speed up analysis.

References

[1] L. Yuan and Y. Y. Lu, "A recursive-doubling Dirichlet-to-Neumann-map method for periodic waveguides," *J. Lightw. Technol.*, vol. 25, no. 11, pp. 3649–3656, Nov. 2007.

[2] E. Ozbay, "Plasmonics: Merging photonics and electronics at nanoscale dimensions," *Science*, vol. 311, no. 5758, pp. 189–193, 2006.

[3] D. K. Gramotnev and S. I. Bozhevolnyi, "Plasmonics beyond the diffraction limit," *Nature Photon.*, vol. 4, no. 2, pp. 83–91, 2010.

[4] J. Shibayama, A. Nomura, R. Ando, J. Yamauchi, and H. Nakano, "A frequency-dependent LOD-FDTD method and its application to the analyses of plasmonic waveguide devices," *IEEE J. Quantum Electron.*, vol. 46, no. 1, pp. 40–49, Jan. 2010.

[5] G. Veronis and S. Fan, "Theoretical investigation of compact couplers between dielectric slab waveguides and two-dimensional metal-dielectric-metal plasmonic waveguides," *Opt. Exp.*, vol. 15, no. 3, pp. 1211–1221, 2007.

[6] H. Zhang, J. Mu, and W.-P. Huang, "Assessment of rational approximations for square root operator in bidirectional beam propagation method," *J. Lightw. Technol.*, vol. 26, no. 5, pp. 600–607, Mar. 2008.

[7] P. L. Ho and Y. Y. Lu, "A stable bidirectional propagation method based on scattering operators," *IEEE Photon. Technol. Lett.*, vol. 13, no. 12, pp. 1316–1318, Dec. 2001.

[8] Y. Y. Lu, "A complex coefficient rational approximation of $\sqrt{1+x}$," *Appl. Numerical Math.*, vol. 27, no. 2, pp. 141–154, 1998.

[9] S. S. A. Obayya, "Novel finite element analysis of optical waveguide discontinuity problems," *J. Lightw. Technol.*, vol. 22, no. 5, pp. 1420–1425, May 2004.

[10] J. Xiao, S. Wu, and X. Sun, "A stable and accurate preconditioner for bidirectional beam propagation method," *IEEE J. Quantum Electron.*, vol. 51, no. 4, pp. 1–7, Apr. 2015.

[11] H. Zhang, J. Mu, and W.-P. Huang, "Analysis of Bragg gratings for long-range surface plasmon polaritons using the bidirectional beam propagation method based on scattering operators," *Proc. SPIE*, vol. 6641, 2007, Art. no. 66 411Z.

[12] J. Mu, H. Zhang, and W.-p. Huang, "Investigation of long-range surface plasmon polaritons gratings by complex mode matching method," *Proc. SPIE*, vol. 6642, 2007, Art. no. 664 213.

[13] S. S. A. Obayya, *Computational Photonics*. New York, NY, USA: Wiley, 2010.

[14] M. Rajarajan, S. Obayya, B. Rahman, K. Grattan, and H. El-Mikali, "Characterisation of low-loss waveguide bends with offset-optimisation for compact photonic integrated circuits," *IEE Proc. Optoelectron.*, vol. 147, no. 6, pp. 382–388, Dec. 2000.

[15] N. Higham, *Functions of Matrices: Theory and Computation (Series SIAM e-books)*. Philadelphia, PA, USA: SIAM, 2008.

[16] Y.-P. Chiou and H.-C. Chang, "Analysis of optical waveguide discontinuities using the Padé approximants," *IEEE Photon. Technol. Lett.*, vol. 9, no. 7, pp. 964–966, Jul. 1997.

[17] E. Deadman, N. Higham, and R. Ralha, "Blocked Schur algorithms for computing the matrix square root," in *Proc. 11th Int. Conf. Appl. Parallel Scientific Comput.*, 2013, vol. 7782, pp. 171–182.

[18] A. M. Said and S. Obayya, "Efficient analysis of electron waveguides with multiple discontinuities," *Opt. Quantum Electron.*, vol. 47, pp. 1–6, 2014.

[19] F. A. Milinazzo, C. A. Zala, and G. H. Brooke, "Rational square-root approximations for parabolic equation algorithms," *J. Acoust. Soc. Amer.*, vol. 101, no. 2, pp. 760–766, 1997.

[20] E. Palik, *Handbook of Optical Constants of Solids (Academic Press Handbook Series)*. New York, NY, USA: Academic, 1998, vol. 3.

[21] T. Tran and S. Kim, "Stability condition of finite-element beam propagation methods in lossy waveguides," *IEEE J. Quantum Electron.*, vol. 50, no. 10, pp. 808–814, Oct. 2014.

[22] G. Veronis, Ş. E. Kocabaş, D. A. Miller, and S. Fan, "Modeling of plasmonic waveguide components and networks," *J. Comput. Theoretical Nanosci.*, vol. 6, no. 8, pp. 1808–1826, 2009.

[23] T. Søndergaard, S. I. Bozhevolnyi, and A. Boltasseva, "Theoretical analysis of ridge gratings for long-range surface plasmon polaritons," *Phys. Rev. B*, vol. 73, Jan. 2006, Art. no. 045320.

[24] S. I. Bozhevolnyi, A. Boltasseva, T. Søndergaard, T. Nikolajsen, and K. Leosson, "Photonic bandgap structures for long-range surface plasmon polaritons," *Opt. Commun.*, vol. 250, no. 4–6, pp. 328–333, 2005.